Cyclic hydroxamic acids derived from α-amino acids
1. Regioselective synthesis, structure, NO-donor and antimetastatic activities of spirobicyclic hydroxamic acids derived from glycine and DL-alanine

I. V. Vystorop,[a] N. P. Konovalova,[a] Yu. V. Nelyubina,[b] V. N. Varfolomeev,[a] B. S. Fedorov,[a] T. E. Sashenkova,[a] E. N. Berseneva,[a] K. A. Lyssenko,[b] and R. G. Kostyanovsky[c]*

[a]*Institute of Problems of Chemical Physics, Russian Academy of Sciences, 1 prosp. Akad. Semenova, 142432 Chernogolovka, Moscow Region, Russian Federation. Fax: +7 (496) 515 5420. E-mail: vystorop@icp.ac.ru*

[b]*A. N. Nesmeyanov Institute of Organoelement Compounds, Russian Academy of Sciences, 28 ul. Vavilova, 119991 Moscow, Russian Federation. Fax: +7 (499) 135 5085. E-mail: kostya@xrlab.ineos.ac.ru*

[c]*N. N. Semenov Institute of Chemical Physics, Russian Academy of Sciences, 4 ul. Kosygina, 119991 Moscow, Russian Federation. Fax: +7 (499) 137 8284. E-mail: kost@center.chph.ras.ru*

The reactions of glycine hydroxamic and DL-alanine hydroxamic acids with triacetonamine are chemoselective and afford 1-hydroxy-7,7,9,9-tetramethyl-1,4,8-triazaspiro[4.5]decan-2-one (**3**) and (±)-1-hydroxy-3,7,7,9,9-pentamethyl-1,4,8-triazaspiro[4.5]decan-2-one (**4**), respectively. The X-ray diffraction study showed that compound **3** crystallizes as a solvate with MeCN (1 : 1). As shown by ESR measurements, spiro hydroxamic acids **3** and **4** are NO donors in *in vitro* biological systems. The NO-donor activity of compounds **3** and **4** was found to be substantially higher in the presence of DMSO. Homologue **4** is a stronger NO donor than **3**. Compound **4** also exhibits high antimetastatic activity (81%) on the B16-melanoma model.

Key words: cyclic hydroxamic acids, amino acids, NO donors, X-ray diffraction study, ESR spectra, B16 melanoma.

Hydroxamic acids (HA, R´CONROH) exhibit a broad spectrum of biological activities,[1] in particular, they inhibit experimental tumor growth.[2] Hydroxamic acids are also known as inhibitors of metalloenzymes (for example, of matrix metalloproteinases[3] and histone deacetylases[4]) involved in various pathophysiological processes. In addition, under particular conditions, HA generate nitric oxide (NO)[1,5] involved in different biological processes,[6] including malignant tumor development.[7]

Previously, we have shown that the reactions of glycine hydroxamic (GlyHA) and DL-alanine hydroxamic (DL-AlaHA) acids with simple ketones afford 3-hydroxyimidazolidin-4-one derivatives **1a—f** (see Refs 8 and 9) and **2**,[10] respectively. Like the reactions of β-alanine hydroxamic acid with ketones,[11] the above-mentioned reactions involve the chemoselective *N,N´*-type cyclocondensation giving rise to cyclic hydroxamic acids (CHA). The structures of monocyclic HA **1a** (see Ref. 8) and **2** (see Ref. 10) and spirobicyclic HA **1e** (see Ref. 9) were established by X-ray diffraction.

In the present study,[12] we examined the possibility of performing the regioselective synthesis of spirobicyclic HA

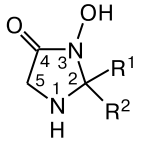

1a—f

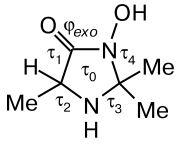

(±)-**2**

1	R^1	R^2	**1**	R^1	R^2	**1**	R^1—R^2
a	Me	Me	**c**	Me	Bu^t	**e**	$(CH_2)_4$
b	Me	Et	**d**	Me	Ph	**f**	$(CH_2)_5$

of this series using the cyclocondensation of GlyHA and DL-AlaHA with functional γ-amino ketone, *viz.*, triacetonamine (TAA), and made a comparative estimate of the activity of the homologues as NO donors and inhibitors of experimental tumor metastasis to reveal the structure—activity relationship.

The choice of TAA as the reaction component was determined by the following factors: 1) the presence of an additional endocyclic amino group leads to an increase in the solubility of the resulting CHA in water; 2) the combination of the lipophilic tetramethyl-substituted piperidine

Published in Russian in *Izvestiya Akademii Nauk. Seriya Khimicheskaya,* No. 1, pp. 127—134, January, 2010.

1066-5285/10/5901-0127

heterocycle and the hydrophilic hydroxamic group in the molecule should increase the amphiphilicity of CHA, thus facilitating the transport of the molecule through biological membranes; 3) the restriction of the conformational flexibility of CHA molecules due to the presence of the spirobicyclic system is favorable for the affinity of CHA as a ligand for its biological target or the activating system and assists in modeling the activity of CHA;[3] 4) the use of symmetrical ketones in the reaction with AlaHA excludes the formation of an additional asymmetric center and, correspondingly, diastereomeric reaction products.

Results and Discussion

Synthesis of and spectroscopic data for acids 3 and 4. The reactions of GlyHA and DL-AlaHA with TAA were found to give homological spirobicyclic HA **3** and **4**, respectively (Scheme 1), like the reactions of GlyHA and DL-AlaHA with trivial ketones.[8—10] The reactions occur under relatively mild conditions, give products in high yields (75 and 80%, respectively), and are self-catalyzed in EtOH (like the reactions giving rise to **1a—f** in MeOH (27—55%)[8,9] or **2** in an excess of ketone (83%)[10]). The mechanism of this type of reactions has been considered earlier.[9]

Scheme 1

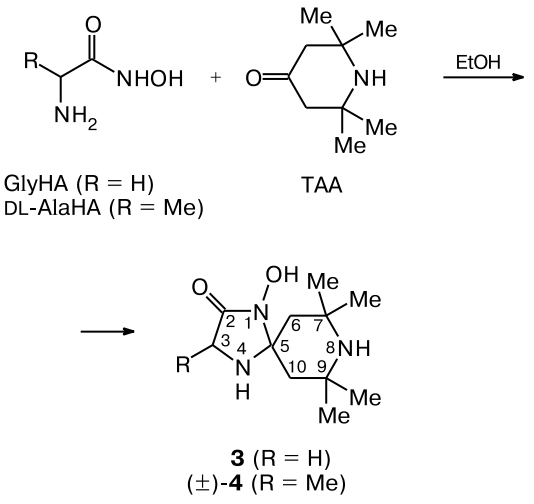

3 (R = H)
(±)-**4** (R = Me)

The structures of CHA **3** and **4** were confirmed by IR and NMR spectroscopy (*cf.* Refs 8 and 9 for **1a—f**). Broadened bands at 2800—2550 cm^{-1} in the IR spectra (KBr) and the positive test reactions with $FeCl_3$ confirm the presence of the exocyclic OH group in compounds **3** and **4**. This is indicative of the *N,N´*-type cyclocondensation giving rise to CHA (—CO—NR—OH), unlike the possible alternative *N,O*-type cyclocondensation producing cyclic hydroxamate (—CO—NH—OR).

In the ^{13}C NMR spectra, the chemical shifts of the carbon atom C(5) of compounds **3** (δ_C 79.6) and **4** (δ_C 80.3) correspond to the tetrahedral rather than to the trigonal configuration of the carbon atom.[8,11] This confirms the spirobicyclic structure of the reaction products and rules out the structure of the corresponding azomethines.[9]

The ^1H and ^{13}C NMR spectra of compounds **3** and **4** (in CD_3OD or DMSO-d_6) show no signals of azomethine forms, which rules out the ring-chain tautomerism slow on the NMR time scale.[11] The tautomerism between the hydroxy amide and hydroxy nitrone forms (O=C—N—OH $\rightleftharpoons$ HO—C=N→O) of acids **3** and **4** fast on the NMR time scale is not observed as well. This is evident from a comparison of the chemical shifts of the carbonyl carbon atoms in the ^{13}C NMR spectra of compounds **3** (DMSO-d_6, δ_C, 171.2) and **4** (CD_3OD, δ_C, 174.4) and the corresponding model compounds existing in fixed tautomeric forms, *viz.* 1,2,2,5,5-pentamethyl-3-methoxyimidazolidin-4-one (O=C—N—OMe, DMSO-d_6, δ_C 170.1; MeOH, δ_C 171.1) and its 4-methoxynitrone form (MeO—C=N→O, DMSO-d_6, δ_C 150.5; MeOH, δ_C 156.7).[13]

X-ray diffraction study of acid 3. The elemental analysis and the ^1H and ^{13}C NMR spectra showed that CHA **3** was prepared as an individual compound, whereas CHA **4** was isolated as a crystal solvate with dioxane (in a ratio of 2 : 1). The crystallization of **3** from MeCN afforded transparent crystals, which are (before drying *in vacuo*) a solvate with MeCN (in a ratio of 1 : 1), as was estabilised by X-ray diffraction (Fig. 1).

As a continuation of our research on the structures of 3-hydroxyimidazolidin-4-one derivatives,[8,9] in the present study we investigated the structure of acid **3** and compared it with the previously studied analogs of the glycine series (acid **1a** (see Ref. 8) and **1e** (see Ref. 9)). (For convenience of the comparison, we used the common atomic numbering scheme for the heterocycles in **1a, 1e**, and **3** (see Fig. 1)).

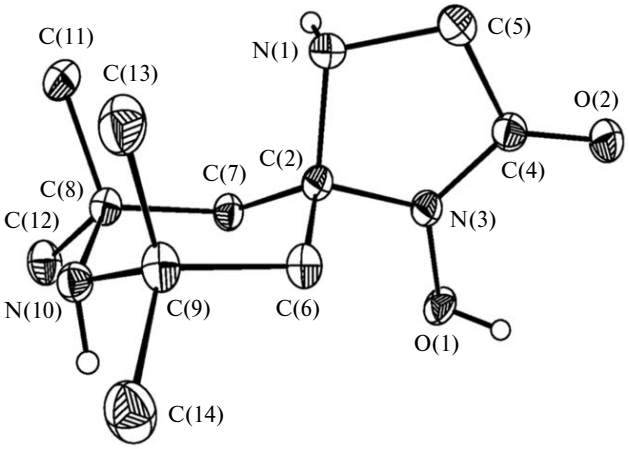

Fig. 1. Molecular structure of formally achiral acid **3** (illustrated by the (*1R*)-configurational enantiomer) with displacement ellipsoids drawn at the 50% probability level.

The conformation of the five-membered ring can quantitatively be estimated from the following ring-puckering parameters:[14] the pseudorotation phase angle (P) and the puckering amplitude (τ_m) can be calculated, in particular, from the endocyclic torsion angles (τ_0—τ_4). The phase angle reflects also the chirality of the five-membered ring[15] of the N type (North, $P_N = 0(360) \pm 90°$, $\tau_2 > 0$) or the S type (South, $P_S = 180 \pm 90°$, $\tau_2 < 0$).

According to this analysis, the imidazolidine ring of the enantiomeric N type in the structures of the previously studied CHA **1a** ($P_N = 44.4°$, $\tau_m = 31.4°$)[8] and **1e** ($P_N = 43.8°$, $\tau_m = 33.7°$)[9] adopts the conformation intermediate between the ideal envelope ${}_{C(2)}E$ ($P_N = 54°$, $\tau_1 = 0$, $|\tau_0| = \tau_2$, $|\tau_3| = \tau_4 = \tau_m$) characteristic of imidazolidines in the isolated state[16] and the ideal half-chair ${}^{N(1)}{}_{C(2)}T$ ($P_N = 36°$, $\tau_0 = \tau_1 < 0$, $\tau_2 = \tau_4 > 0$, $\tau_3 < 0$, $|\tau_3| = \tau_m$) (Scheme 2). Correspondingly, the S-type heterocycle of molecules **1a** and **1e** in the crystal structures has the enantiomeric form intermediate between the envelope conformation ${}^{C(2)}E$ ($P_S = 234°$, $\tau_1 = 0$, $\tau_0 = |\tau_2|$, $\tau_3 = |\tau_4| = \tau_m$) and the half-chair conformation ${}^{C(2)}{}_{N(1)}T$ ($P_S = 216°$, $\tau_0 = \tau_1 > 0$, $\tau_2 = \tau_4 < 0$, $\tau_3 > 0$, $\tau_3 = \tau_m$).[8,9] By contrast, the less puckered ($\tau_m = 28.8°$) N-type enantiomeric form of the imidazolidine heterocycle ($P_N = 33.0°$) in **3** (see Fig. 1) corresponds almost exactly to the conformation ${}^{N(1)}{}_{C(2)}T$, but it is slightly distorted toward the ideal envelope ${}^{N(1)}E$ ($P_N = 18°$, $\tau_0 = 0$, $|\tau_1| = \tau_4$, $\tau_2 = |\tau_3| = \tau_m$), the latter being the conformation that is typical of the γ-lactam ring in the crystals.[17] Correspondingly, the S-type enantiomeric form of the heterocycle in acid **3** ($P_S = 213°$) is close to the conformation ${}^{C(2)}{}_{N(1)}T$ and is distorted toward the conformation ${}_{N(1)}E$ ($P_S = 198°$, $\tau_0 = 0$, $\tau_1 = |\tau_4|$, $|\tau_2| = \tau_3 = \tau_m$).

Scheme 2

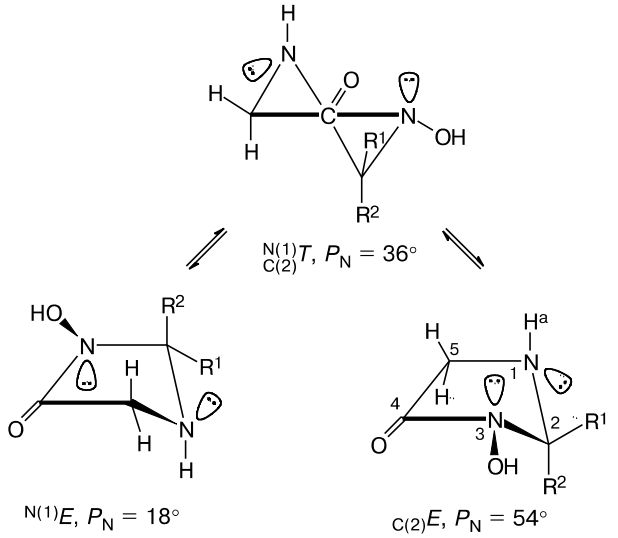

The characteristic feature of the molecular structure of **3** in the crystal is also that the hydroxamic fragment O(1)—N(3)—C(4)—O(2) ($\varphi_{exo} = 4.4(2)°$, Table 1) and the joint endocyclic angle C(2)—N(3)—C(4)—C(5) ($\tau_0 = -8.1°$, see Table 1) are less twisted compared to the corresponding substantially nonplanar fragments of molecules **1a** ($\varphi_{exo} = 19.3°$, $\tau_0 = -14.9°$)[8] and **1e** ($\varphi_{exo} = 17.9°$, $\tau_0 = -15.6°$).[9] Unlike **1a** and **1e**, in which the amide nitrogen atom is slightly pyramidalized[8,9] ($\Sigma\omega N(3) = 350.8°$ (**1a**) and 350.9° (**1e**)), the amide nitrogen atom in molecule **3** has a virtually planar configuration ($\Sigma\omega N(3) = 358.8°$, Table 2). As a consequence, the exocyclic O(1)—N(3)—C(2) and O(1)—N(3)—C(4) bond angles in molecule **3** are larger (see Table 2) than the corresponding angles in **1a** (117.7(2)° and 119.7(2)°, respectively)[8] and **1e** (118.1(1)° and 120.0(1)°).[9] A larger increase in the O(1)—N(3)—C(4) bond angle compared to the O(1)—N(3)—C(2) bond angle in molecule **3** is apparently associated with the fact that the flattening of the O=C—N—O fragment leads to an increase in the torsion-

Table 1. Selected torsion angles in molecule **3**

Angle	Value//deg
C(5)—N(1)—C(2)—N(3) (τ_3)	–27.5(2)
C(2)—N(1)—C(5)—C(4) (τ_2)	24.2(2)
C(6)—C(2)—C(7)—C(8) (ϕ_0)	52.8(2)
C(7)—C(2)—C(6)—C(9) (ϕ_1)	–51.7(2)
O(1)—N(3)—C(4)—O(2) (φ_{exo})	4.4(2)
N(3)—C(4)—C(5)—N(1) (τ_1)	–10.2(2)
C(2)—N(3)—C(4)—C(5) (τ_0)	–8.1(2)
C(2)—C(6)—C(9)—N(10) (ϕ_2)	47.8(2)
N(1)—C(2)—N(3)—C(4) (τ_4)	22.9(2)
C(2)—C(7)—C(8)—N(10) (ϕ_5)	–49.9(2)
C(7)—C(8)—N(10)—C(9) (ϕ_4)	47.4(2)
C(6)—C(9)—N(10)—C(8) (ϕ_3)	–46.4(2)

Table 2. Bonds angles in molecule **3**

Angle	ω/deg	Angle	ω/deg
C(2)—N(1)—C(5)	105.5(1)	C(7)—C(8)—C(11)	112.5(1)
N(1)—C(2)—N(3)	101.6(1)	C(7)—C(8)—C(12)	109.1(1)
N(1)—C(2)—C(6)	112.9(1)	C(11)—C(8)—C(12)	108.0(1)
N(1)—C(2)—C(7)	113.6(1)	N(10)—C(8)—C(11)	111.1(1)
N(3)—C(2)—C(6)	108.2(1)	N(10)—C(8)—C(12)	105.5(1)
N(3)—C(2)—C(7)	109.9(1)	C(6)—C(9)—N(10)	110.6(1)
C(6)—C(2)—C(7)	110.1(1)	C(6)—C(9)—C(13)	111.9(1)
O(1)—N(3)—C(2)	120.5(1)	C(6)—C(9)—C(14)	109.2(1)
O(1)—N(3)—C(4)	124.6(1)	N(10)—C(9)—C(13)	111.2(1)
C(2)—N(3)—C(4)	113.7(1)	N(10)—C(9)—C(14)	105.4(1)
O(2)—C(4)—N(3)	126.8(1)	C(13)—C(9)—C(14)	108.3(1)
O(2)—C(4)—C(5)	127.8(1)	C(8)—N(10)—C(9)	118.6(1)
N(3)—C(4)—C(5)	105.4(1)	C(2)—N(1)—H(1N)	106.8
N(1)—C(5)—C(4)	106.0(1)	C(5)—N(1)—H(1N)	104.0
C(2)—C(6)—C(9)	114.9(1)	C(8)—N(10)—H(10N)	105.5
C(2)—C(7)—C(8)	114.7(1)	C(9)—N(10)—H(10N)	104.2
C(7)—C(8)—N(10)	110.4(1)	N(1S)—C(1S)—C(2S)	178.4(2)

al strain and the dipole-dipole repulsion between the *cis*-oriented dipoles of the exocyclic C=O and N—O bonds.

It should be noted that the *syn*-periplanar (*sp*) twist of the hydroxamic fragment in **1a**, **1e**, and **3**, as opposed to acyclic[18] hydroxamic acids, is responsible for the helical chirality of *P*-type (plus, $\varphi_{exo} > 0$) or *M*-type (minus, $\varphi_{exo} < 0$) molecules[19] associated with the chirality of the enantiomeric conformation of the N-type ($\tau_2 > 0$) or S-type ($\tau_2 < 0$) imidazolidine ring, respectively.

A decrease in the twisting of the hydroxamic fragment and an increase in the planarity of the amide atom N(3) in **3** should be accompanied by an increase in the n_N-π^*(C=O)-amide conjugation, which is reflected in a considerable elongation of the O(2)=C(4) bond and a shortening of the N(3)—C(4) bond in molecule **3** (Table 3) compared to **1a** (1.225(3) and 1.343(3) Å, respectively)[8] and **1e** (1.218(2) and 1.342(2) Å),[9] as well as to the mean C=O bond length (1.232(1) Å) in the planar amide group of γ-lactams in crystals.[17]

According to the classical theory of resonance (O=C—NR—OH ↔ O^-—C=NR^+—OH), the strengthening of the n_N-π^*(C=O)-amide conjugation is accompanied by an increase in the positive charge on the nitrogen atom, which should, in turn, lead to the strengthening of the bond between the N(3) atom and the more electronegative O(1) atom and the weakening of the bond between this nitrogen atom and the less electronegative C(2) atom.[20] Actually, the corresponding changes in the O(1)—N(3) and C(2)—N(3) bond lengths are observed in the structure of **3** (Table 3) compared to the analogous bond lengths in **1a** (1.394(3) and 1.484(3) Å, respectively)[8] and **1e** (1.391(1) and 1.474(2) Å).[9] It should be noted that the C(2)—N(3) bond in molecules **1a**, **1e**, and **3** is substantially longer than the mean N—C_β bond (1.455(1) Å) in γ-lactams in crystals,[17] which is also attributed to the contribution of the $n_{N(1)}$—$\sigma^*_{C(2)-N(3)}$ anomeric interaction[17] with the involvement of the pseudoequatorial (pseudo-*e*) lone pair (LP) of the N(1) atom (φ ($LP_{N(1)}$—N(1)—C(2)—N(3)) = −152.5° (**1a**),[8] −157° (**1e**),[9] −152.4° (**3**)).

Interestingly, the imidazolidine ring in molecule **3** is characterized by a decrease in the endocyclic bond angles (C(2)—N(3)—C(4) and N(3)—C(4)—C(5)) and by an increase in the exocyclic bond angles (O(2)—C(4)—N(3) and O(2)—C(4)—C(5)) (see Table 2) compared to the corresponding mean bond angles in the γ-lactam ring in the crystals (ω(C_β—N—C(O)) = 114.9(1)°, ω(N—C(O)—C_α) = = 108.4(1)°, ω(O=C—N) = 125.8(1)°, ω(O=C—C_α) = 125.7(1)°).[17]

Table 3. Bond lengths in molecule **3**

Bond	*d*/Å	Bond	*d*/Å
O(1)—N(3)	1.375(2)	C(7)—C(8)	1.537(2)
N(1)—C(2)	1.473(2)	C(8)—N(10)	1.504(2)
N(1)—C(5)	1.478(2)	C(8)—C(11)	1.534(2)
O(2)=C(4)	1.242(2)	C(8)—C(12)	1.534(2)
C(2)—N(3)	1.491(2)	C(9)—N(10)	1.506(2)
C(2)—C(6)	1.534(2)	C(9)—C(13)	1.529(2)
C(2)—C(7)	1.525(2)	C(9)—C(14)	1.531(2)
N(3)—C(4)	1.337(2)	N(1S)—C(1S)	1.138(2)
C(4)—C(5)	1.519(2)	C(1S)—C(2S)	1.458(2)

Another consequence of the change in the conformation of the imidazolidine ring and a decrease in the twisting of the hydroxamic fragment is that the mutual *trans* orientation of the polar N(1)—C(2) and N(3)—O(1) bonds (φ(N(1)—C(2)—N(3)—O(1)) = −169.5°) in **3** substantially differs from the corresponding parameters in molecules **1a** (175.2°)[8] and **1e** (177.2°)[9] of the same chirality in the crystals. The mutual orientation of LP of the nitrogen atoms N(1) and N(3) (φ($LP_{N(1)}$—N(1)...N(3)—$LP_{N(3)}$) = = 155(1)°) in **3** is similar to the corresponding pseudotorsion angles in **1a** (154°)[8] and **1e** (150°)[9] and corresponds to the favorable antiperiplanar (*ap*) orientation of LP of the geminal nitrogen atoms in aminals.[21] It is interesting that the mutual *trans* orientation of the dipoles of another pair of the polar bonds (φ(O(2)—C(4)—C(5)—N(1)) = = 170.4°) stabilizing the conformation of the heterocycle in **3** undergoes much lesser changes compared to **1a** (174.9°)[8] or **1e** (174.5°).[9]

The piperidine ring of compound **3** in the crystal structure adopts a nearly ideal chair conformation (*cf.*, ϕ_0—ϕ_5, Table 1; φ(C(11)—C(8)...C(9)—C(13)) = 0.3(1)°, φ(C(12)—C(8)...C(9)—C(14)) = 1.0(1)°) and, according to the general rule, is orthogonal to the imidazolidine ring (φ(C(5)—N(1)—C(2)—C(6)) = = 88.2(2)°, φ(C(6)—C(2)—N(3)—C(4)) = −96.2(2)°), like the cyclopentane ring in **1e** (87.2° and −89.8°, respectively).[9]

According to the known Thorpe—Ingold effect,[22] the fact that the endocyclic C(8)—N(10)—C(9) bond angle in the six-membered ring is larger than the endocyclic C(2)—N(1)—C(5) bond angle in the five-membered ring of molecule **3** (see Table 2) corresponds to a decrease in the degree of pyramidalization of the amine nitrogen atom N(10) (ΣωN(10) = 328.3°, see Table 2) compared to the amine nitrogen atom N(1) (ΣωN(1) = 316.3°, see Table 2) exhibiting similar pyramidalization in molecules **1a** (317.2°)[8] and **1e** (315.0°).[9] The corresponding decrease in the basicity of the N(1) atom compared to the N(10) atom (due to the stronger *s* character of *pseudo-e*-$LP_{N(1)}$ than that of *pseudo-e*-$LP_{N(10)}$, φ(C(7)—C(8)—N(10)—$LP_{N(10)}$) = = 174(1)°, φ(C(6)—C(9)—N(10)—$LP_{N(10)}$) = −173(1)°) of molecule **3** in the crystal leads to a decrease in the proton-withdrawing ability of the N(1) atom compared to the N(10) atom. Apparently, this fact facilitates the formation of the strong intermolecular O(1)—H(1O)...N(10) hydrogen bond (Table 4, Fig. 2), as opposed to the structures of **1a** and **1e**, in which there is the strong intermolecular O(1)—H(1O)...N(1) hydrogen bond (*d*(O(1)...N(1)) =

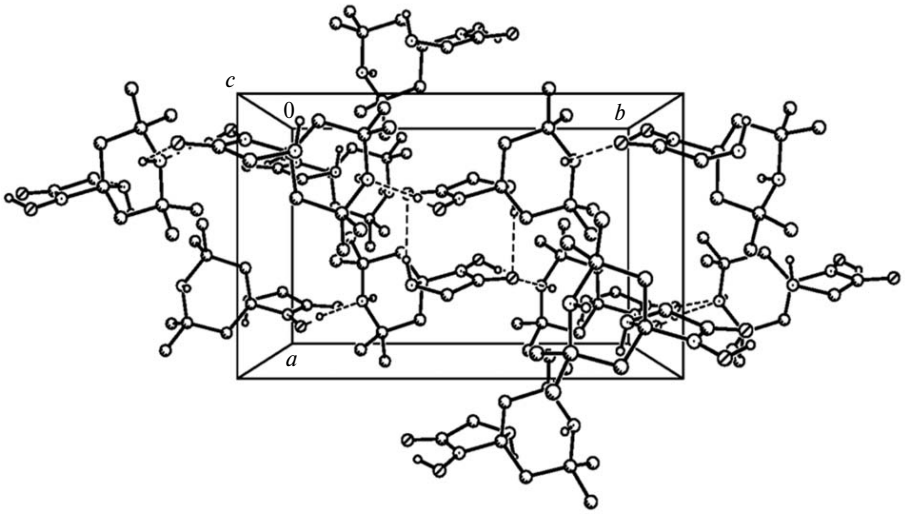

Fig. 2. Fragment of the crystal packing of acid **3** projected onto the crystallographic plane *ab*. The hydrogen atoms, which are not involved in hydrogen bonding, are not shown. The hydrogen bonds are indicated by dashed lines. The geometric parameters of the intermolecular hydrogen bonds are given in Table 4.

= 2.679 and 2.693 Å, respectively).[8,9] The N(1) atom, which competes with N(10) as the acceptor of the proton H(1O), does not form hydrogen bonds with protons in the crystal structure of **3**.

According to the above-considered scheme of resonance, an increase in the amide conjugation in the hydroxamic fragment should also lead to an increase in the negative charge on the carbonyl oxygen atom O(2), which increases its proton-withdrawing ability. Apparently, this facilitates the involvement of the carbonyl oxygen atom into two weak intermolecular N—H...O=C hydrogen bonds with the *pseudo-a* protons H(1N) (φ(H(1N)—N(1)—C(2)—N(3)) = 83(1)°, φ(H(1N)—N(1)—C(5)—C(4)) = –88(1)°) and H(10N) (φ(C(11)—C(8)—N(10)—H(10N)) = 166(1)°, φ(C(13)—C(9)—N(10)—H(10N)) = = –165(1)°) of both endocyclic amino groups in the crystal structure of **3** (see Table 4, Fig. 2). In addition, the proton H(10N) is involved in the intermolecular N(10)—H(10N)...N≡C—Me hydrogen bond with the solvent molecule (see Table 4).

Table 4. Parameters of D—H...A hydrogen bonds formed by molecules **3** in the crystal structure

D—H	A	*d*(D—H)	*d*(H...A)	*d*(D...A)	ω(D—H...A)
		Å			/deg
O(1)—H(1O)	N(10)^{i}	0.81	1.76	2.563(2)	170
N(1)—H(1N)	O(2)^{ii}	0.89	2.28	3.146(2)	163
N(10)—H(10N)	O(2)^{iii}	0.90	2.54	3.053	116
N(10)—H(10N)	N(1S)	0.90	2.54	3.355(2)	151

Note. Symmetry codes: (*i*) 0.5 – *x*, –0.5 + *y*, 1.5 – *z*; (*ii*) –*x* + 1, –*y* + 1, –*z* + 1; (*iii*) 0.5 – *x*, 0.5 + *y*, 1.5 – *z*.

As a consequence of the increase in the amide resonance and the involvement of the carbonyl group in two intermolecular hydrogen bonds, the stretching vibrations of this group in the IR spectrum (KBr) of **3** ($\nu_{(C=O)}$ = 1669 and 1652 cm^{-1}) are lower than those of **1a** ($\nu_{(C=O)}$ = = 1697 cm^{-1})[8] and **1e** ($\nu_{(C=O)}$ = 1716 and 1696 cm^{-1}),[9] which is evidence of a strengthening of hydrogen bonds with the carbonyl group.

Like in the crystal structures of **1a**[8] and **1e**,[9] the intramolecular O(1)—H(10)...O(2)=C(4) hydrogen bond in the crystal structure of **3** is absent (*d*(H(10)...O(2)) = 2.866(2) Å) because the O(1)—H(1O) bond is non-coplanar with the plane of the amide group (φ(H(1O)—O(1)—N(3)—C(4) = = 30(1)°).

A comparison of the crystal structures of monocyclic HA **1a** (space group $P2_12_12_1$, $Z = 4$)[8] and **2** ($P2_1/c$, $Z = 8$)[10] and spirobicyclic HA **1e** ($P2_1/n$, $Z = 4$)[9] shows that these structures have an identical system of intermolecular hydrogen bonds, *viz.*, a strong O—H...N(1) hydrogen bond and a weak N(1)—H(1N)...O=C hydrogen bond. At the same time, the presence of the additional donor-withdrawing NH group results in a different system of intermolecular hydrogen bonds in the crystal structure of acid **3** ($P2_1/n$, $Z = 4$).

Thus, the weak intermolecular N(1)—H(1N)...O=C hydrogen bond and the strong intermolecular O—H...N(1) hydrogen bond in the crystal structure of spirobicyclic HA **1e** (see Ref. 8) give rise to infinite chains formed by the homochiral and heterochiral molecules, respectively. However, in the crystal structure of spirobicyclic HA **3**, pairs of the weak N(1)—H(1N)...O=C hydrogen bonds are involved in the formation of racemic dimers (Fig. 3), whereas the strong intermolecular O—H...N(10) hydrogen bond and the N(10)—H(10N)...O=C hydrogen bond

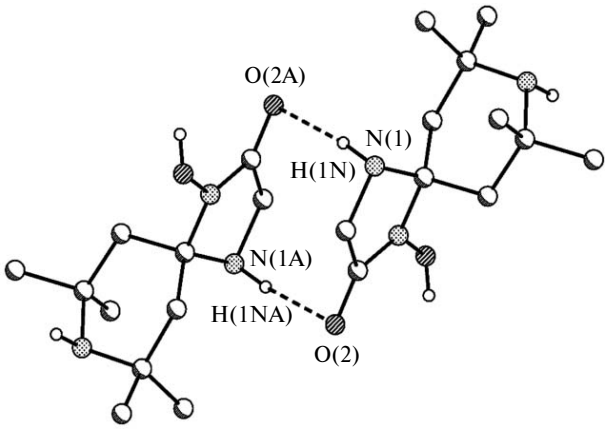

Fig. 3. Centrosymmetric dimer formed through the C=O...H(1N) bond in the crystal structure of acid **3**. The atoms labeled A are related to the unlabeled atoms by the symmetry operation $-x + 1, -y + 1, -z + 1$.

give rise to infinite chains formed by the molecules of the same chirality (Fig. 4).

Investigation of the NO-donor activity of acids 3 and 4. Previously, the ability of hydroxamic acids (as exemplified by aceto- and aromatic HA)[5] to release NO in *in vitro* biological systems has been demonstrated by the NO-mediated activation of the iron-containing enzyme guanylate cyclase by measuring the activity of the enzyme[5a] or the relaxation of the rat aorta.[5b] It was also shown that NO produced during metabolism of organic nitrates in liver tissues of animals is bound by iron-containing proteins of this biological system to form, in particular, heme iron nitrosyl complexes (heme NO complexes),[23a] which are detected by ESR spectra swith the characteristic triplet splitting and the g factor of the signal equal to 2.01.[23]

In the present study, the NO-generating activity of CHA **3** and **4** in *in vitro* biological systems was investigated[24] by ESR spectroscopy. The ESR spectra of samples, which were obtained by the incubation of the biomass (liver tissues of animals) with aqueous solutions of CHA **3** or **4**, show a weak signal of the heme NO complex with the

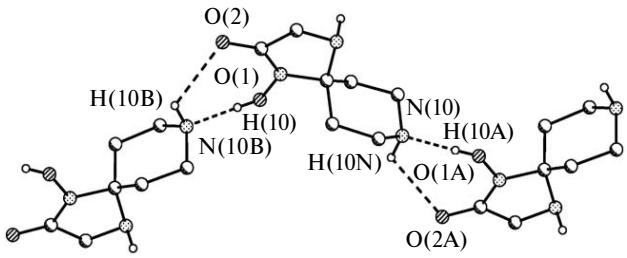

Fig. 4. Homochiral chain formed through O—H...N(10) and C=O...H(10N) bonds in the crystal structure of acid **3**. The atoms labeled A and B are related to the unlabeled atoms by the symmetry operations $0.5 - x$, $0.5 + y$, $1.5 - z$ and $0.5 - x$, $-0.5 + y$, $1.5 - z$, respectively. The methyl groups are omitted.

g factor of 2.007 complicated by the superposition with the stronger signal of flavo- and ubisemiquinones ($g = 2.003$). The low intensity of the ESR signal of the heme NO complexes, which has the maximum value for samples incubated for 3 h, is indicative of the weak NO-donor activity of acids **3** and **4** in an aqueous medium of the biological systems. At the same time, samples, which were prepared by the addition of solutions of **3** or **4** in DMSO to the biomass followed by the incubation for 3 h, give much more intense (by almost an order of magnitude) signals of the heme NO complexes (Fig. 5) compared to samples of the biological systems incubated in an aqueous medium during the same period of time. This is indicative of a substantial increase in the NO generation by acids **3** and **4** in the biological system containing DMSO (~10% v/v) compared to the NO generation by these acids in an aqueous medium of the biological system. Apparently, this effect is associated with an increase in the membranotropic activity[6a] or the oxidative[5a] biotransformation of compounds **3** and **4** in the biological system in the presence of DMSO. It should be noted that the NO-donor activity of acid **4** is ~60% higher than that of **3** (see Fig. 5).

Evaluation of the of antitumor and antimetastatic activities of acids 3 and 4. Previously, it has been shown for organic nitrates[25] that NO donors can enhance the antitumor activity of known cytostatic agents and inhibit the experimental tumor metastasis. In the present study, we examined the antitumor and antimetastatic activities of acids **3** and **4** on the tumor models P388 leukemia and B16 melanoma, respectively.

Actually, the combined use of acid **3** (or **4**) and an antitumor cytostatic agent results in an increase in the

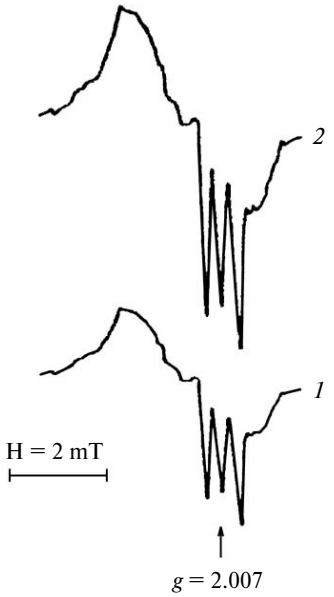

Fig. 5. ESR spectra of samples of the biomass after 3 h incubation with solutions of acids **3** (*1*) and **4** (*2*) in DMSO at the final concentration of $5 \cdot 10^{-3}$ mol L^{-1}.

Table 5. Antileukemic effect of the combined action of acids **3** and **4** and antitumor cytostatic agents on the P388 leukemia model

Agent	Time of administration/days	Dose /mg kg^{-1}	ILS* (%)
3	1—7	330	2.8
Cisplatin	1—7	1.2	157
3 + Cisplatin	1—7	330 + 1.2	224
Doxorubicin	1—7	1.5	108
3 + Doxorubicin	1—7	330 + 1.5	141
4	1—7	400	0
Methotrexate	1—7	1.0	118
4 + Methotrexate	1—7	400+1.0	183

* ILS is the increase in the average life span.

antileukemic activity of the latter by 30—55% compared to its individual inhibiting activity (Table 5).

A comparative evaluation of the antimetastatic activity of non-toxic compounds **3** and **4** showed that the racemic acid of the alanine series (**4**) much actively inhibits the metastasis of B16 melanoma (the index of metastasis inhibition (IMI), 81%) than the achiral acid of the glycine series (**3**) (IMI, 12%) (Fig. 6).

To sum up, we showed that the reactions of GlyHA and DL-AlaHA with triacetonamine occur analogously to the reactions with simple ketones *via* the *N,N´*-type chemoselective cyclocondensation. According to the X-ray diffraction data and the IR and NMR spectra, acids **3** and **4** in crystals and in solution, like the previously studied compounds **1a—f** (see Refs 8 and 9) and **2** (see Ref. 10) of this class, exist in the hydroxyamide tautomeric form, the hydroxynitrone or azomethine tautomeric forms being virtually absent.

It was shown for the first time that CHA 3-hydroxyimidazolidin-4-ones are NO donors and inhibitors of experimental tumor metastasis, CHA of the alanine series being more active than the homologue of the glycine series.

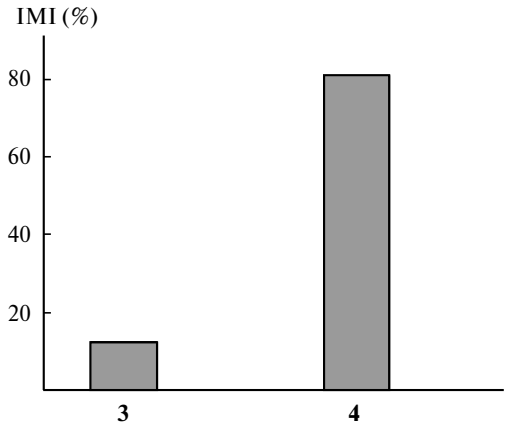

Fig. 6. Inhibition of experimental B16 melanoma metastasis during therapy with acids **3** and **4** (the dose was 200 mg kg^{-1}; the times of administration were 2—8 days).

Experimental

The IR spectra of samples pressed in KBr pellets were recorded on a Specord-82M spectrophotometer in the 400—4000 cm^{-1} range. The NMR spectra were measured on a Bruker WM-400 spectrometer operating at 400.14 MHz (^{1}H) and a Bruker AC-200 spectrometer operating at 50.32 MHz (^{13}C). The ^{1}H and ^{13}C chemical shifts were measured with respect to $SiMe_4$ and the solvent, respectively, as the internal standard. The melting points were determined on a Boetius micro hot-stage apparatus. The elemental analysis was carried out in the Analytical Laboratory of the Institute of Problems of Chemical Physics of the Russian Academy of Sciences. The ESR spectra were recorded at 77 K on a Varian E-104 spectrometer at a microwave power of 10 mW with 1 mT modulation of magnetic field. The solvents were purified and dried according to standard procedures. The starting compounds, *viz.*, aminoacetic acid *N*-hydroxyamide (GlyHA) and DL-2-aminopropionic acid *N*-hydroxyamide (DL-AlaHA), were synthesized according to known procedures.[26]

Synthesis of hydroxamic acids 3 and 4 (general method). The hydroxamic acid GlyHA or DL-AlaHA (30 mmol) was added to a solution of triacetonamine (2,2,6,6-tetramethylpiperidin-4-one) (38 mmol) in anhydrous EtOH (70 mL). The resulting suspension was refluxed until the reagent was dissolved (1—1.5 h). Then the mixture was cooled to 20°C and passed through a thin layer of Al_2O_3 (neutral, Brockman II). The solvent was evaporated *in vacuo*. The residue was crystallized from MeCN (or dioxane) and dried *in vacuo* (1 Torr).

1-Hydroxy-7,7,9,9-tetramethyl-1,4,8-triazaspiro[4.5]decan-2-one (3). The yield was 75%, white powder, m.p. 148—150 °C (from MeCN). Found (%): C, 57.92; H, 9.09; N, 18.78. $C_{11}H_{21}N_3O_2$. Calculated (%): C, 58.12; H, 9.31, N, 18.49. IR (KBr), ν/cm^{-1}: 3302 (NH), 3030 (NH), 2988 (CH), 2959 (CH), 2940 (CH), 2860 (CH), 2758 (br, OH), 2665 (br, OH), 2600 (br, OH), 1669 (C=O), 1652 (sh, C=O), 1504, 1456, 1448, 1379, 1358, 1349, 1241, 1221, 1204, 1168, 1068, 849, 668. ^{1}H NMR (CD_3OD), δ: 1.21 (s, 6 H, 2 Me); 1.45 (s, 6 H, 2 Me); 1.62 (d, 2 H, $C\underline{H}_AH_BCMe_2$, ^2J = 13.6 Hz); 1.75 (d, 2 H, $CH_A\underline{H}_BCMe_2$, ^2J = 13.6 Hz); 3.32 (s, 2 H, CH_2N). ^{1}H NMR (DMSO-d_6), δ: 1.09 (s, 6 H, 2 Me); 1.28 (s, 6 H, 2 Me); 1.40 (d, 2 H, $C\underline{H}_AH_BCMe_2$, ^2J = 13.5 Hz); 1.45 (d, 2 H, $CH_A\underline{H}_BCMe_2$, ^2J = 13.5 Hz); 3.10 (m, 3 H, $C\underline{H}_2N\underline{H}$). ^{13}C NMR (DMSO-$d_6$), δ: 29.2 (q, 2 C, $C\underline{Me}_AMe_B$, ^1J = 126.8 Hz); 35.3 (q, 2 C, $CMe_A\underline{Me}_B$, ^1J = 124.6 Hz); 41.3 (t, 2 C, CH_2, ^1J = 129.8 Hz); 45.1 (t, CH_2N, ^1J = 142.9 Hz); 50.3 (m, 2 C, $\underline{C}Me_2$); 79.6 (m, NCN); 171.2 (m, C=O).

(±)-1-Hydroxy-3,7,7,9,9-pentamethyl-1,4,8-triazaspiro-[4.5]decan-2-one (4). The yield was 80%, white powder (solvate with dioxane in a stoichiometric ratio of 2 : 1), m.p. 110—112 °C (from dioxane). Found (%): C, 59.07; H, 9.87; N, 14.95. $C_{12}H_{23}N_3O_2{\cdot}0.5C_4H_8O_2$. Calculated (%): C, 58.92; H, 9.54; N, 14.72. IR (KBr), ν/cm^{-1}: 3274 (NH); 3039 (NH); 2962 (CH); 2934 (CH); 2869 (CH); 2795 (br, OH); 2665 (br, OH); 2611 (br, OH); 1680 (sh, C=O); 1670 (C=O); 1660 (sh, C=O); 1536, 1487, 1456, 1371, 1361, 1227, 1204, 1122, 1104, 998. ^{1}H NMR (CD_3OD), δ: 1.19 (s, 3 H, Me_A); 1.22 (s, 3 H, Me_B); 1.31 (d, 3 H, $CH\underline{Me}$, ^3J = 7.1 Hz); 1.45 (s, 3 H, Me_C); 1.48 (s, 3 H, Me_D);

1.62 (s, 2 H, CH_2, $\Delta\nu_{AB} \to 0$); 1.63 (d, 1 H, C<u>H</u>$_A$H$_B$, ^2J = 13.1 Hz); 1.89 (d, 1 H, CH$_A$<u>H</u>$_B$, ^2J = 13.1 Hz); 3.45 (q, 1 H, C<u>H</u>Me, ^3J = 7.0 Hz); 3.65 (s, 4 H, dioxane). ^{1}H NMR (DMSO-d_6), δ: 0.99 (s, 3 H, Me$_A$); 1.01 (s, 3 H, Me$_B$); 1.17 (d, 3 H, CH<u>Me</u>, ^3J = 7.0 Hz); 1.28 (s, 3 H, Me$_C$); 1.30 (s, 3 H, Me$_D$); 1.32 (d, 1 H, C<u>H</u>$_A$H$_B$, ^2J = 13.5 Hz); 1.40 (d, 1 H, CH$_A$<u>H</u>$_B$, ^2J = 13.5 Hz); 1.47 (d, 1 H, C<u>H</u>$_C$H$_D$, ^2J = 13.6 Hz); 1.57 (d, 1 H, CH$_C$<u>H</u>$_D$, ^2J = 13.6 Hz); 2.61 (d, 1 H, NH, ^3J = 10.1 Hz); 3.23 (m, 1 H, C<u>H</u>Me); 3.55 (s, 4 H, dioxane). ^{13}C NMR (CD_3OD), δ: 17.4 (dq, CH<u>Me</u>, ^1J = 127.7 Hz, ^2J = 3.8 Hz); 28.6 (qm, C<u>Me</u>$_A$, ^1J = 126.8 Hz); 28.8 (qm, C<u>Me</u>$_B$, ^1J = 126.8 Hz); 34.7 (qm, C<u>Me</u>$_C$, ^1J = 125.1 Hz); 34.9 (qm, C<u>Me</u>$_D$, ^1J = 125.1 Hz); 40.8 (t, CH_2, ^1J = 126.8 Hz); 45.3 (t, CH_2, ^1J = 126.8 Hz); 53.0 (dq, <u>C</u>HMe, ^1J = 144.9 Hz, ^2J = 4.0 Hz); 53.2 (br.s, 2 C, 2 <u>C</u>Me$_2$); 68.4 (s, dioxane); 80.3 (m, NCN); 174.4 (m, C=O).

X-ray diffraction study was carried out at 120 K, crystals of **3** ($C_{11}H_{21}N_3O_2 \cdot C_2H_3N$, M = 268.36) were grown by crystallization from acetonitrile, monoclinic, space group $P2_1/n$, a = 8.3539(4), b = 13.5768(7), c = 12.6197(7) Å, β = 90.263(5)°, V = 1431.30(13) Å^3, Z = 4 (Z' = 1), d_{calc} = 1.245 g cm^{-3}, μ(MoKα) = 0.86 cm^{-1}, F(000) = 584. The intensities of 20893 reflections were measured at 120 K on a SMART 1000 CCD diffractometer (λ(MoKα) = 0.71072 Å, ω-scanning technique, 2θ < 58°), and 3802 independent reflections (R_{int} = 0.0293) were used in the refinement. The structure was solved by direct methods and refined by the full-matrix least-squares method with anisotropic displacement parameters based on F^2_{hkl}. The hydrogen atoms of OH and NH groups were located in difference Fourier maps. The H(C) atoms were positioned geometrically. All hydrogen atoms were refined isotropically using a riding model. The final R factors for **3** were R_1 = 0.0526 (calculated based on F_{hkl} for 2990 reflections with $I > 2\sigma(I)$), wR_2 = 0.1353 (calculated based on F^2_{hkl} for all 3802 reflections), the number of refined parameters was 173, GOOF = 1.002. The calculations were carried out with the use of the SHELXTL 5.10 program package.[27]

Studies of the NO-donor activity of acids **3** and **4** *in vitro* were carried out on liver tissues of Balb mice with a weight of 22—25 g, which were housed in a vivarium and provided water and food *ad libitum*. Mice were sacrificed by cervical dislocation. The liver was removed, sliced, and incubated with solutions of acids **3** and **4** in water or DMSO at room temperature to reach the final concentration in the biological system of $5 \cdot 10^{-3}$ mol L^{-1} and 10% (v/v) DMSO. Aliquots of liver tissues incubated with aqueous solutions of acids **3** and **4** were taken each hour for 5 h; aliquots incubated with solutions of these acids in DMSO were taken at one hour intervals for 3 h. These aliquots were used to prepare samples (d = 4 mm, h = 20 mm) according to a known procedure[28] at 77 K for ESR measurements. The degree of NO generation was estimated from the intensity of the signal of the heme iron nitrosyl complexes in the ESR spectra.

Investigation of the antitumor and antimetastatic activities of acids **3** and **4** was carried out using the tumor models P388 leukemia and B16 melanoma, respectively, on BDF hybrid mice. The tumor transplantation was performed according to a standard procedure.[29] Mice were injected intraperitoneally with aqueous solutions of the samples. The doses and the times of administration are given in Table 5 and Fig. 6. The overall toxicity (LD_{50}) was determined on BDF hybrid mice with a single injection of aqueous solutions of acids **3** and **4**. The antileukemic activity was assessed from the increase in the average life span (ILS (%) = 100(T/T_c — 1)), where T and T_c are the measured average life span (in days) of mice of the experimental and control groups, respectively. The B16 melanoma-bearing mice were sacrificed 24 days after the tumor inoculation, the number of lung metastases was calculated, and the index of metastasis inhibition (IMI) was evaluated as IMI (%) = 100[1 — $(A \cdot B)/(A_c \cdot B_c)$], where A and A_c are the frequency of metastasis in the experimental and control groups, respectively, B and B_c are the average number of metastases in the experimental and control groups, respectively.

References

1. C. J. Marmion, D. Griffith, K. B. Nolan, *Eur. J. Inorg. Chem.*, 2004, 3003; D. Griffith, K. Krot, J. Comiskey, K. B. Nolan, C. J. Marmion, *Dalton Trans.*, 2008, **1**, 137.
2. R. Hoekstra, F. A. L. M. Eskens, J. Verweij, *Oncologist*, 2001, 6, 415; M. Hidalgo, S. G. Eckhardt, *J. Natl. Cancer Inst.*, 2001, **93**, 178; J. B. Nielands, *Science*, 1967, **156**, 1443.
3. M. Whittaker, C. D. Floyd, P. Brown, A. J. H. Gearing, *Chem. Rev.*, 1999, **99**, 2735.
4. T. A. Miller, D. J. Witter, S. Belvedere, *J. Med. Chem.*, 2003, **46**, 5097.
5. (a) L. N. Koikov, N. V. Alexeeva, E. A. Lisitza, E. S. Krichevsky, N. B. Grigoryev, A. V. Danilov, I. S. Severina, N. V. Pyatakova, V. G. Granik, *Mendeleev Commun.*, 1998, 165; (b) C. J. Marmion, T. Murphy, J. R. Docherty, K. B. Nolan, *Chem Commun.*, 2000, 1153.
6. (a) V. G. Granik and N. B. Grigor´ev, *Oksid azota (NO): novyi put´ k poisku lekarstv* [*Nitric Oxide (NO). New Route to Drug Design*], Vuzovskaya kniga, Moscow, 2004, 360 pp. (in Russian); (b) A. R. Butler and R. Nicholson, *Life, Death and Nitric Oxide*, RS·C, Cambridge, 2003, 250p.
7. N. P. Konovalova, *Tekhnologii zhivykh sistem* [*Technology of Living Systems*], 2004, **1**, 42 (in Russian); J. M. Fukuto, L. J. Ignarro, *Acc. Chem. Res.*, 1997, 149.
8. I. V. Vystorop, K. A. Lyssenko, R. G. Kostyanovsky, *Mendeleev Commun.*, 2002, 85.
9. I. V. Vystorop, K. A. Lyssenko, V. N. Voznesensky, V. P. Lodygina, R. G. Kostyanovsky, *Mendeleev Commun.*, 2002, 193.
10. I. V. Vystorop, Z. G. Aliev, N. Yu. Andreeva, L. O. Atovmyan, B. S. Fedorov, *Izv. Akad. Nauk, Ser. Khim.*, 2000, 180 [*Russ. Chem. Bull., Int. Ed.*, 2000, **49**, 182].
11. O. A. Luk´yanov, P. B. Gordeev, *Izv. Akad. Nauk, Ser. Khim.*, 1998, 691 [*Russ. Chem. Bull.* (*Engl. Transl.*), 1998, **47**, 669].
12. I. V. Vystorop, N. P. Konovalova, T. E. Sashenkova, B. S. Fedorov, *Tez. dokl. IX Nauchnoi shkoly-konf. po organicheskoi khimii* [*Abstrs. of Papers, IX Scientific School-Conf. on Organic Chemistry*] (*December 11—15, 2006, Moscow*), Moscow, 2006, p. 114 (in Russian).
13. G. I. Shchukin, I. A. Grigor´ev, L. B. Volodarskii, *Khim. Geterotsikl. Soedin.*, 1990, 478 [*Chem. Heterocycl. Compd.* (*Engl. Transl.*), 1990, **26**, 409].
14. C. Altona, M. Sundaralingam, *J. Am. Chem. Soc.*, 1972, **94**, 8205; C. Mathe, C. Perigand, *Eur. J. Org. Chem.*, 2008, 1489.
15. I. V. Vystorop, A. Rauk, C. Jaime, I. Dinares and R. G. Kostyanovsky, *Khim. Geterotsikl. Soedin.*, 1995, 1479 [*Chem. Heterocycl. Compd.* (*Engl. Transl.*),1995, **31**, 1280].
16. A. Skancke, L. Vilkov, *Acta Chem. Scand.*, 1988, **42A**, 717.
17. L. Norskov-Lauritsen, H.-B. Burgi, P. Hofmann, H. R. Schmidt, *Helv. Chim. Acta*, 1985, **68**, 76.

18. L. Bauer, O. Exner, *Angew. Chem., Int. Ed.*, 1974, **13**, 376.
19. R. S. Cahn, C. K. Ingold, V. Prelog, *Angew. Chem., Int. Ed.*, 1966, **5**, 385.
20. S. A. Glover, A. Rauk, *J. Org. Chem.*, 1999, **64**, 2340.
21. A. Alexakis, A. Tomassini, C. Chouillet, S. Roland, P. Mangeney, G. Bernardinelli, *Angew. Chem., Int. Ed.*, 2000, **39**, 4093.
22. R. M. Beesley, C. K. Ingold, J. F. Thorpe, *J. Chem. Soc.*, 1915, **107**, 1080; T. Ohwada, H. Hirao, A. Ogawa, *J. Org. Chem.*, 2004, **69**, 7486.
23. (a) O. L. Belaya, L. M. Baider, Z. V. Kuropteva, *Byull. Eksp. Biol. Meditsiny*, 2006, **142**, 403 [*Bull. Exp. Biol. Medicine* (*Engl. Transl.*), 2006, **142**]; (b) S. Archer, *FASEB J.*, 1993, **7**, 349.
24. V. N. Varfolomeev, N. P. Konovalova, B. S. Fedorov, T. E. Sashenkova, S. V. Blokhina, I. V. Vystorop, *Tez. dokl. V natsional´noi nauchno-prakticheskoi konferentsii s mezhdunarodnym uchastiem "Aktivnye formy kisloroda, oksid azota, antioksidanty i zdorov´e cheloveka"* [*Abstrs. of Papers, V All-Russian Scientific Practical Conference with International Participation "Active Forms of Oxygen, Nitric Oxide, Antioxidants, and Human Health"*] *(September 18—22, 2007, Smolensk)*, Smolensk, 2007, p. 14 (in Russian).
25. N. P. Konovalova, S. A. Goncharova, L. M. Volkova, T. A. Rajewskaya, L. T. Eremenko, A. M. Korolev, *Nitric Oxide: Biology and Chemistry*, 2003, **8**, 59.
26. K. G. Cunningham, G. T. Newbold, F. S. Spring, J. Stark, *J. Chem. Soc.,* 1949, 2091.
27. G. M. Sheldrick, *SHELXTL v. 5.10, Structure Determination Software Suit*, Bruker AXS, Madison, Wisconsin, USA.
28. G. N. Bogdanov, V. N. Varfolomeev, V. M. Pavlova, N. M. Emanuel´, *Dokl. Akad. Nauk SSSR*, 1976, **226**, 207 [*Dokl. Chem.* (*Engl. Transl.*), 1976, **226**].
29. *Eksperimental´naya otsenka protivoopukholevykh preparatov v SSSR i SShA* [*Experimental Evaluation of Antitumor Drugs in the USSR and USA*], Eds Z. P. Sofina, A. B. Syrkin (USSR), A. Goldin, A. Klein (USA), Meditsina, Moscow, 1980, 296 pp. (in Russian).

Received December 30, 2008